

Synthesis, Structure, and Hydride–Deuteride Exchange Studies of CpMoH₃(PMe₂Ph)₂ and Theoretical Studies of the CpMoH₃(PMe₃)₂ Model System

Fatima Abugideiri, James C. Fettinger, Brett Pleune, and Rinaldo Poli*[†]

Department of Chemistry and Biochemistry, University of Maryland,
College Park, Maryland 20742

Craig A. Bayse and Michael B. Hall*

Department of Chemistry, Texas A&M University, College Station, Texas 77843

Received May 14, 1996[⊗]

The synthesis and characterization of CpMoH₃(PMe₂Ph)₂, **1**, is described. Compound **1** is obtained from the reaction between CpMoCl₃, PMe₂Ph, and LiAlH₄, in 61% yield. Compound **1** has also been obtained from the reaction of CpMo(*o*-C₆H₄PMe₂)(PMe₂Ph)₂ with H₂. Characterization of **1** by ¹H- and ³¹P-NMR spectroscopies shows a high degree of fluxionality for the hydride atoms, even at low temperatures. A single-crystal X-ray structure indicates that the geometry is pseudo-octahedral, with a relative *mer* arrangement of the three H ligands and the two PMe₂Ph ligands occupying relative *trans* positions. This is in contrast with the only other previously reported structure of a Mo(IV) trihydride, Cp*MoH₃(dppe), which adopts a pseudo trigonal prismatic structure. The Mo–P (average 2.41(8) Å) and Mo–H distances (average 1.64(4) Å) are similar to those found in Cp*MoH₃(dppe). The closest H–H distance is 1.79 Å, consistent with a classical hydride. The results of *ab initio* calculations for the CpMoH₃(PMe₃)₂ model in different configurations agree with the experimental observations and suggest that a mechanism of hydride exchange consisting of a Bailar twist, which interconverts pseudo-octahedral *mer*, *trans* and *fac* geometries, is possible. The process of hydride–deuteride exchange of **1** in C₆D₆ is also examined.

Introduction

Transition metal polyhydride systems have been the focus of much recent attention. The determination of classical and nonclassical hydrides,^{1–3} the mechanism of hydride fluxionality,⁴ and other studies on oxidation^{5–15}

or protonation^{16–25} of these systems have been reported in recent years. The (ring)MH₃L₂ polyhydride system (M = Mo or W) has been known since 1979²⁶ but has not been the subject of detailed studies. In particular, no structural information was reported until the recent investigation of Cp*MoH₃(dppe) in our laboratory,²⁷ which was determined to be pseudotrigonal prismatic, contrary to the expected pseudo-octahedral structure. A mechanism of hydride scrambling was proposed based on the interconversion between the pseudo trigonal prismatic and pseudo-octahedral geometries. In order

[†] Current address: Laboratoire de Synthèse et d'Électrosynthèse Organométallique, Faculté des Sciences "Gabriel", 6, Boulevard Gabriel, 21100 Dijon, France. E-mail: Rinaldo.Poli@u-bourgogne.fr.

[⊗] Abstract published in *Advance ACS Abstracts*, February 15, 1997.

(1) Hamilton, D. G.; Crabtree, R. H. *J. Am. Chem. Soc.* **1988**, *110*, 4126–4133.

(2) Luo, X.-L.; Crabtree, R. H. *Inorg. Chem.* **1990**, *29*, 2788–2791.

(3) Van Der Sluys, L. S.; Eckert, J.; Eisenstein, O.; Hall, J. H.; Huffman, J. C.; Jackson, S. A.; Koetzle, T. F.; Kubas, G. J.; Vergamini, P. J.; Caulton, K. G. *J. Am. Chem. Soc.* **1990**, *112*, 4831–4841.

(4) Lee, J. C., Jr.; Yao, W.; Crabtree, R. H.; Rügger, H. *Inorg. Chem.* **1996**, *35*, 695–699.

(5) Klinger, R. J.; Huffman, J. C.; Kochi, J. K. *J. Am. Chem. Soc.* **1980**, *102*, 208–216.

(6) Allison, J. D.; Cameron, C. J.; Wild, R. E.; Walton, R. A. *J. Organomet. Chem.* **1981**, *218*, C62–C66.

(7) Rhodes, L. F.; Zubkowski, J. D.; Folting, K.; Huffman, J. C.; Caulton, K. G. *Inorg. Chem.* **1982**, *21*, 4185–4192.

(8) Bruno, J. W.; Caulton, K. G. *J. Organomet. Chem.* **1986**, *315*, C13–C16.

(9) Dettly, M. R.; Jones, W. D. *J. Am. Chem. Soc.* **1987**, *109*, 5666–5673.

(10) Costello, M. T.; Walton, R. A. *Inorg. Chem.* **1988**, *27*, 2563–2564.

(11) Herrmann, W. A.; Theiler, H. G.; Herdtweck, E.; Kiprof, P. *J. Organomet. Chem.* **1989**, *367*, 291–311.

(12) Bianchini, C.; Laschi, F.; Peruzzini, M.; Ottaviani, F.; Vacca, A.; Zanello, P. *Inorg. Chem.* **1990**, *29*, 3394–3402.

(13) Roullier, L.; Lucas, D.; Mugnier, Y.; Antiñolo, A.; Fajardo, M.; Otero, A. *J. Organomet. Chem.* **1991**, *412*, 353–362.

(14) Westerberg, D. E.; Rhodes, L. F.; Edwin, J.; Geiger, W. E.; Caulton, K. G. *Inorg. Chem.* **1991**, *30*, 1107–1112.

(15) Zlota, A. A.; Tilset, M.; Caulton, K. G. *Inorg. Chem.* **1993**, *32*, 3816–3821.

(16) Adams, G. S. B.; Green, M. L. H. *J. Chem. Soc., Dalton Trans.* **1981**, 353–356.

(17) Bruno, J. W.; Huffman, J. C.; Caulton, K. G. *J. Am. Chem. Soc.* **1984**, *106*, 1663–1669.

(18) Parkin, G.; Bercaw, J. E. *J. Chem. Soc., Chem. Commun.* **1989**, 255–257.

(19) Kim, Y.; Deng, H.; Meek, D. W.; Wojcicki, A. *J. Am. Chem. Soc.* **1990**, *112*, 2798–2800.

(20) Cazanoue, M.; He, Z.; Neibecker, D.; Mathieu, R. *J. Chem. Soc., Chem. Commun.* **1991**, 307–309.

(21) Earl, K. A.; Jia, G.; Maltby, P. A.; Morris, R. H. *J. Am. Chem. Soc.* **1991**, *113*, 3027–3039.

(22) Christ, M. L.; Sabo-Etienne, S.; Chaudret, B. *Organometallics* **1994**, *13*, 3800–3804.

(23) Lemke, F. R.; Brammer, L. *Organometallics* **1995**, *14*, 3980–3987.

(24) Rothfuss, H.; Gusev, D. G.; Caulton, K. G. *Inorg. Chem.* **1995**, *34*, 2894–2901.

(25) Shubina, E. S.; Krylov, A. N.; Belkova, N. V.; Epstein, L. M.; Borisov, A. P.; Mahaev, V. D. *J. Organomet. Chem.* **1995**, *493*, 275–277.

(26) Aviles, T.; Green, M. L. H.; Dias, A. R.; Romao, C. *J. Chem. Soc., Dalton Trans.* **1979**, 1367–1371.

(27) Fettinger, J. C.; Pleune, B.; Poli, R. *J. Am. Chem. Soc.* **1996**, *118*, 4906.

to establish whether the unexpected pseudo trigonal prismatic geometry is the result of electronic or steric factors, we have synthesized and crystallographically characterized a less sterically hindered compound of this genre, namely $\text{CpMoH}_3(\text{PMe}_2\text{Ph})_2$, **1**. As will be shown here, the geometry of this compound corresponds to the originally anticipated pseudo-octahedral geometry. The hypothesis of a pseudo trigonal prismatic–pseudo-octahedral interconversion as a mechanism of hydride scrambling will be examined in more detail and supported by theoretical calculations on model systems in both geometries. We also report here on the slow H/D exchange for **1** in C_6D_6 , which gives rise to distinct ^1H -NMR hydride resonances for all $\text{CpMoH}_n\text{D}_{3-n}(\text{PMe}_2\text{Ph})_2$ species ($n = 3, 2, 1$).

Experimental Section

All manipulations were carried out under an inert atmosphere of nitrogen or argon by the use of vacuum-line, Schlenk, syringe, or drybox techniques. Solvents were dried by conventional methods and distilled under nitrogen prior to use. Deuterated solvents were dried over molecular sieves and degassed by three freeze–pump–thaw cycles prior to use. Methanol was degassed by three freeze–pump–thaw cycles prior to use. ^1H -, ^2H -, and $^{31}\text{P}\{^1\text{H}\}$ -NMR measurements were made on Bruker AF200, WP200, or AM400 spectrometers; the peak positions are reported with positive shifts downfield of TMS (^1H , ^2H), as calculated from the residual solvent peaks (^1H) or from external D_2O (^2H), and downfield of external 85% H_3PO_4 (^{31}P). For each ^{31}P -NMR spectrum, a sealed capillary containing H_3PO_4 was immersed in the same NMR solvent used for the measurement and this was used as the reference. The standard inversion–recovery–pulse sequence $180-\tau-90$ was used to determine T_1 . Values of T_1 were obtained from the slopes of linear plots of $\ln(2I_{\text{eq}}/(I_{\text{eq}} - I_t))$ vs τ , where I_{eq} is the peak intensity at $\tau = \infty$. PMe_2Ph (Strem Chemical Co.) and LiAlH_4 (Aldrich) were used without further purification. CpMoCl_3 ²⁸ and $\text{CpMo}(\sigma\text{-C}_6\text{H}_4\text{PMe}_2)(\text{PMe}_2\text{Ph})_2$ ²⁹ were prepared according to literature procedures.

Synthesis of $\text{CpMoH}_3(\text{PMe}_2\text{Ph})_2$ (1**).** To a suspension of 810 mg of CpMoCl_3 (3.03 mmol) in 50 mL of THF was added 1.045 mL of PMe_2Ph (7.57 mmol). The suspension rapidly dissolved and turned red-brown. One gram of LiAlH_4 (24.0 mmol) was slowly added, as a powder, to the solution. The solution immediately turned orange-yellow. After the addition was complete, the mixture was stirred for 60 min. Methanol (10 mL) was then added dropwise at 0 °C, resulting in vigorous evolution of H_2 . After H_2 evolution ceased, the solvent was evaporated under vacuum and the resulting residue was extracted into heptane (150 mL). The heptane solution was filtered and concentrated to ca. 5 mL. The solution began to develop an orange precipitate; the mixture was stored at -80 °C for 12 h. The solution was filtered, and the microcrystalline precipitate was washed with cold (-80 °C) heptane. The solid was dried in vacuo. Yield: 816 mg (61%). This crude solid proved to be a mixture of compounds **1** and $\text{CpMoH}_5(\text{PMe}_2\text{Ph})_2$ (**2**) by ^1H -NMR: the pentahydride byproduct constituted less than 12% of the material by NMR integration. Pure **1** was obtained by recrystallization from a saturated solution of heptane, affording orange-purple crystals. One of the crystals obtained in this manner was used for the X-ray analysis.

^1H -NMR of **1** (C_6D_6): δ 7.65–7.08 (m, 10H, Ph), 4.25 (s, 5H, Cp), 1.62 (d, 12H, Me, $J_{\text{PH}} = 7.6$ Hz), -5.14 (t, 3H, M–H, $J_{\text{PH}} = 40.5$ Hz). ^{31}P -NMR (C_6D_6): δ 36.3 (s, PMe_2Ph). ^1H -NMR of **2** (C_6D_6): δ 7.68–7.02 (m, 5H, Ph), 4.86 (s, 5H, Cp), 1.55 (d,

6H, $J_{\text{PH}} = 9.8$ Hz), -4.18 (d, 5H, $J_{\text{PH}} = 52.0$ Hz). ^{31}P -NMR (C_6D_6): δ 26.9 (s, PMe_2Ph).

Reaction of $\text{CpMoCl}_2(\text{PMe}_2\text{Ph})_2$ with LiAlH_4 . Formation of **1 and $\text{CpMoH}(\text{PMe}_2\text{Ph})_3$ (**3**).** CpMoCl_2 (83 mg, 0.357 mmol) and 4 equiv of PMe_2Ph (204 μL , 1.428 mmol) were added to 2 mL of toluene. To this mixture, LiAlH_4 (100 mg, 0.263 mmol) was added slowly, as a powder. Over the next 12 h, the yellow-brown starting material slowly dissolved as the solution color changed from red-brown to yellow-brown over a grey precipitate. An aliquot of this solution was filtered, the solvent was removed under reduced pressure, and the residue was redissolved in C_6D_6 for ^1H -NMR analysis, which showed **3** as the major product, as well as another broad triplet resonance centered at $\delta -9.40$ ($J_{\text{PH}} = 22.0$ Hz). The solution was allowed to stir for 1 week, and another aliquot was taken for ^1H -NMR analysis, which showed **1** as the major product with **3** and the broad triplet resonance as minor products. After 2 weeks, MeOH was added to the solution until gas evolution ceased, followed by complete removal of the solvent under reduced pressure. NMR spectroscopy showed a nearly 1:1 mixture of **1** and **2** as the only hydride products. The above reaction was repeated using 2 equiv of PMe_2Ph with similar results. ^1H -NMR of **3** (C_6D_6): δ 7.8–6.9 (m, 15H, Ph), 4.50 (s, 5H, Cp), 1.57 (d, 18H, Me, $J_{\text{PH}} = 6.2$ Hz), -7.68 (q, 1H, M–H, $J_{\text{PH}} = 50.9$ Hz). ^{31}P -NMR (C_6D_6): δ 34.7 (s, PMe_2Ph).

Reaction between $\text{CpMo}(\sigma\text{-C}_6\text{H}_4\text{PMe}_2)(\text{PMe}_2\text{Ph})_2$ and H_2 . Formation of **1 and **3**.** $\text{CpMo}(\sigma\text{-C}_6\text{H}_4\text{PMe}_2)(\text{PMe}_2\text{Ph})_2$ (42 mg, 0.073 mmol) was dissolved in C_6D_6 (1 mL) and introduced in a thin-walled 5 mm NMR tube. After one freeze–pump–thaw cycle, the sample was exposed to H_2 (1 atm) and the tube was flame sealed. This solution was kept at room temperature and exposure to normal laboratory fluorescent light for several days, with ^1H - and ^{31}P -NMR monitoring. The ^1H -NMR spectrum indicated the formation of **3** (initially) and then **1**, followed by H/D exchange at the hydride positions on a longer time scale. Exposure of the solution to UV light accelerated the rate of H/D exchange. Full details are discussed in the Results section. ^1H -NMR resonance for the Mo–H protons in **1**- d_n (δ , C_6D_6): -5.16 (t, $J_{\text{PH}} = 40.5$ Hz, d_0); -5.20 (t, $J_{\text{PH}} = 40.4$ Hz, d_1); -5.24 (t, $J_{\text{PH}} = 39.7$ Hz, d_2). The C_6D_6 solvent was evaporated under reduced pressure, and the residue was redissolved in C_6H_6 for ^2H -NMR spectroscopy. Three broad resonances were observed in the deuteride region of the ^2H -NMR spectrum, centered at $\delta -5.07$, -5.29 , and -5.50 ppm. This reaction was also repeated in toluene- d_8 with identical results, except that the rate of H/D exchange was, in this case, dramatically reduced (see Results section). The solution of **1** and **3** in toluene- d_8 was used for the T_1 measurements.

X-ray Analysis for Compound 1. A reddish-purple crystal with dimensions $0.38 \times 0.25 \times 0.23$ mm was placed and optically centered on the Enraf-Nonius CAD-4 diffractometer. The crystal final cell parameters and crystal orientation matrix were determined from 25 reflections in the range $15.1^\circ < \theta < 19.1^\circ$ and confirmed with axial photographs. The data did not need correction for decay but were corrected for absorption, on the basis of the variation in the intensity of the ψ -scan of eight reflections (transmission factors ranging from 0.5026–0.5524).

On the basis of systematic absences, the space group could be either $C2/c$ (No. 15) or Cc (No. 9). Intensity statistics indicated the former, along with the cell contents requiring eight asymmetric units. Direct methods resulted in the successful location of the Mo and P atoms. The remaining non-hydrogen atoms were found from an initial difference Fourier map. After full-matrix least-squares refinement, all of the hydrogen atoms were directly located. All of the hydrogen atoms were freely refined isotropically, whereas the non-hydrogen atoms were refined anisotropically. A final difference Fourier map was featureless with $|\Delta r| \leq 0.437 \text{ e} \cdot \text{\AA}^{-3}$, indicating that the structure is both correct and complete.

(28) Poli, R.; Kelland, M. A. *J. Organomet. Chem.* **1991**, *419*, 127–136.

(29) Poli, R.; Krueger, S. T.; Abugideiri, F.; Haggerty, B. S.; Rheingold, A. L. *Organometallics* **1991**, *10*, 3041–3046.

Table 1. Crystal Data for Compound 1

mol form	C ₂₁ H ₃₀ MoP ₂
mol wt	440.33
temp	153(2) K
wavelength	0.710 73 Å
cryst syst	monoclinic
space group	C2/c
unit cell dimensions	$a = 24.9623(12)$ Å, $\alpha = 90^\circ$ $b = 7.4092(4)$ Å, $\beta = 113.687(5)^\circ$ $c = 24.423(2)$ Å, $\gamma = 90^\circ$
volume, Z	4136.4(4) Å ³ , 8
density (calcd)	1.414 Mg/m ³
abs coeff	0.789 mm ⁻¹
$F(000)$	1824
cryst size	0.375 × 0.250 × 0.225 mm
θ range for data collection	2.89–24.99°
limiting indices	$-29 \leq h \leq 29$, $0 \leq k \leq 8$, $-14 \leq l \leq 28$
no. of reflns collected	3680
no. of independent reflns	3630 ($R(\text{int}) = 0.0137$)
abs corr	semi-empirical from ψ -scans
max and min transmission	0.5524 and 0.5026
refinement method	full-matrix least-squares on F^2
no. of data/restraints/parameters	3630/0/337
goodness-of-fit on F^2	1.316
final R indices ($I > 2\sigma(I)$)	$R_1 = 0.0292$, $wR_2 = 0.0700$ (3369 data)
R indices (all data)	$R_1 = 0.0327$, $wR_2 = 0.0717$
largest diff peak and hole	0.437 and -0.391 e ⁻ Å ⁻³

Table 2. Selected Bond Distances (Å) and Angles (deg) for Compound 1^a

Mo(1)–C(4)	2.249(3)	Mo(1)–P(1)	2.4038(8)
Mo(1)–C(5)	2.274(4)	Mo(1)–P(2)	2.4095(8)
Mo(1)–C(3)	2.302(3)	Mo(1)–H(1A)	1.68(4)
Mo(1)–C(1)	2.346(3)	Mo(1)–H(1B)	1.65(4)
Mo(1)–C(2)	2.370(4)	Mo(1)–H(1C)	1.58(6)
Mo(1)–CNT	1.975(4)		
P(1)–Mo(1)–P(2)	126.29(3)	H(1A)–Mo(1)–H(1B)	136(2)
P(1)–Mo(1)–H(1A)	82.3(13)	CNT–Mo(1)–P(1)	116.5(1)
P(2)–Mo(1)–H(1A)	83.2(13)	CNT–Mo(1)–P(2)	117.0(1)
P(1)–Mo(1)–H(1B)	78(2)	CNT–Mo(1)–H(1A)	111.4(14)
P(2)–Mo(1)–H(1B)	78(2)	CNT–Mo(1)–H(1B)	112(2)
P(1)–Mo(1)–H(1C)	64(2)	CNT–Mo(1)–H(1C)	178(2)
P(2)–Mo(1)–H(1C)	63(2)		

^a CNT = Cp ring centroid.

Crystal data are reported in Table 1, and selected bond distances and angles are collected in Table 2.

Theoretical Details. Geometry optimizations of CpMoH₃(PMe₂)₂ were performed at the restricted Hartree–Fock (RHF) level of theory. Relative energies of the RHF geometries were recalculated at the MP2 level. The metal basis set was double- ξ with a triple- ξ function for the d orbitals. The ($n + 1$)s and ($n + 1$)p functions of the metal have been included according to recent studies that demonstrate the importance of these functions.^{30,31} The hydride ligands are represented in a triple- ξ basis set.³² The carbons and hydrogens of the Cp ligand and phosphorus are represented by double- ξ functions.³³ Minimal basis sets (STO-3G)³⁴ were used for the carbons and hydrogens of the methyl groups in PMe₃. Effective core potentials represent the inner shells of the molybdenum,³⁵

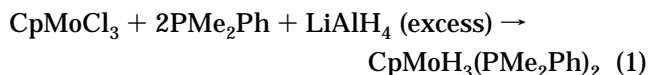
(30) Couty, M.; Hall, M. B. *J. Comput. Chem.* **1996**, *17*, 1359.(31) Couty, M.; Bayse, C. A.; Hall, M. B. *J. Phys. Chem.* **1996**, *100*, 13976.(32) Dunning, T. H. *J. Phys. Chem.* **1970**, *55*, 716.(33) Dunning, T. H. *J. Chem. Phys.* **1970**, *53*, 2823.(34) Hehre, W. J.; Stewart, R. F.; Pople, J. A. *J. Chem. Phys.* **1969**, *51*, 2657. Hehre, W. J.; Ditchfield, R.; Stewart, R. F.; Pople, J. A. *J. Chem. Phys.* **1970**, *52*, 2769. Pietro, W. J.; Hehre, W. J. *J. Comput. Chem.* **1983**, *4*, 241. Collins, J. B.; Schleyer, P. van R.; Binkley, J. S.; Pople, J. A. *J. Chem. Phys.* **1976**, *64*, 5142. Tatewaki, H.; Huzinaga, S. *J. Chem. Phys.* **1980**, *72*, 399.(35) Ross, R. B.; Powers, J. M.; Atashroo, T.; Ermler, W. C.; Lajohn, L. A.; Christiansen, P. A. *J. Chem. Phys.* **1990**, *93*, 6654.

carbon,³⁶ and phosphorus.³⁷ Calculations were performed using the GAMESS-UK package³⁸ on a SGI Power Challenge at the Supercomputer Center of Texas A&M University and on the SP2 at Cornell Theory Center.

Results and Discussion

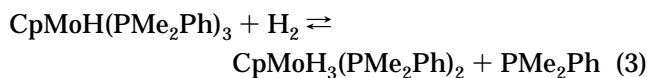
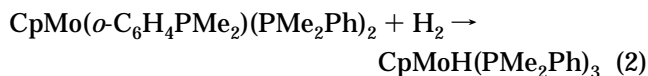
Synthesis and Spectroscopic Characterization.

Compound **1** has been synthesized from the reaction of CpMoCl₃ with LiAlH₄ in THF in the presence of excess PMe₂Ph (eq 1), followed by methanolysis of the reaction mixture. The reaction also gave rise to minor but



significant quantities of a byproduct, which is characterized by a doublet hydride resonance at $\delta -4.18$ ($J_{\text{PH}} = 52.0$ Hz). This is assigned to CpMoH₅(PMe₂Ph), **2**, by analogy with the resonance of Cp*MoH₅(PMe₃), which was reported as a doublet at $\delta -3.17$ ($J_{\text{PH}} = 50.3$ Hz).³⁹ Compound **1**, however, has been obtained pure by low-temperature recrystallization from heptane. Similar compounds, namely ($\eta^5\text{-C}_5\text{H}_4\text{Pr}^i$)MoH₃L₂ (L = PMe₃, PMe₂Ph, or L₂ = Prⁱ₂PCH₂CH₂PPrⁱ₂), have been prepared from Mo(III) precursors, namely ($\eta^5\text{-C}_5\text{H}_4\text{Pr}^i$)-MoCl₂L₂, and LiAlH₄.⁴⁰ Since CpMoCl₂(PMe₂Ph)₂ is known,²⁹ we also explored the utilization of such a starting material by analogy with the strategy reported by Green *et al.*⁴⁰ However, although spectroscopic monitoring shows that compound **1** also forms by this route, a considerable amount of CpMoH(PMe₂Ph)₃, **3**, (quartet hydride resonance at $\delta -7.72$, $J_{\text{PH}} = 50.9$ Hz, *cf.* the resonance for the similar⁴¹ CpMoH(PMe₃)₃ at $\delta -8.37$, $J_{\text{PH}} = 52.6$ Hz) is also generated and the separation of the two compounds is difficult. Longer reaction times led to the disappearance of **3**, but at the same time, considerable amounts of compound **2** were also formed. Overall, the utilization of CpMoCl₃ as a starting material has proven more effective in our hands. Reaction 1 probably proceeds via the formation of the adducts CpMoCl₃(PMe₂Ph)_{*n*} (*n* = 1, 2), as previously reported.⁴²

Yet another route to compound **1** is the reaction between the ortho-metalated complex²⁹ CpMo(*o*-C₆H₄-PMe₂)(PMe₂Ph)₂ and H₂ shown in eqs 2 and 3. The



reaction affords compound **3** initially, but a slow,

(36) Stevens, W. J.; Basch, H.; Krauss, M. *J. Chem. Phys.* **1984**, *81*, 6026.(37) Wadt, W. R.; Hay, P. J. *J. Chem. Phys.* **1985**, *82*, 284–298.(38) Guest, M. F.; Kendrick, J.; van Lenthe, J. H.; Schoeffel, K.; Sherwood, P. *GAMESS-UK*. Computing for Science, Ltd.: Daresbury Laboratory, 1995.(39) Abugideiri, F.; Kelland, M. A.; Poli, R. *Organometallics* **1993**, *12*, 2388–2389.(40) Grebenik, P. D.; Green, M. L. H.; Izquierdo, A.; Mtetwa, V. S. B.; Prout, K. *J. Chem. Soc., Dalton Trans.* **1987**, 9–19.(41) Brookhart, M.; Cox, K.; Cloke, F. G. N.; Green, J. C.; Green, M. L. H.; Hare, P. M.; Bashkin, J.; Derome, A. E.; Grebenik, P. D. *J. Chem. Soc., Dalton Trans.* **1985**, 423–433.(42) Abugideiri, F.; Gordon, J. C.; Poli, R.; Owens-Waltermire, B. E.; Rheingold, A. L. *Organometallics* **1993**, *12*, 1575–1582.

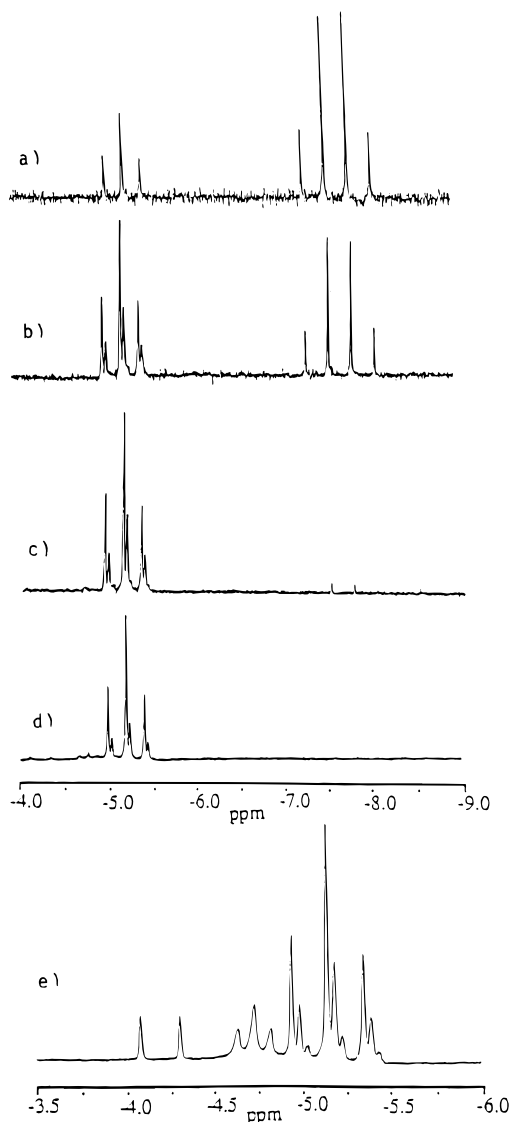


Figure 1. $^1\text{H-NMR}$ spectrum (hydride region) of a mixture of compounds **1** and **3** in C_6D_6 obtained from reactions **2** and **3**: (a) after 7 days at room temperature in a sealed NMR tube, (b) after 13 days at room temperature in a sealed NMR tube, (c) after 29 days at room temperature in a sealed NMR tube, (d) after 13 days on a Schlenk line under H_2 ($P = 1$ atm), (e) as in d, after 30 min of UV irradiation.

temperature-dependent equilibrium with compound **1**, which involves loss of PMe_2Ph , is established later. At room temperature, the reaction eventually proceeds quantitatively to **1**, under an atmosphere of H_2 , but can be reversed by warming. In a sealed NMR tube, the reaction finally arrives at a mixture of **3** (minor) and **1** (major) because of the insufficient amount of H_2 available; when this mixture is warmed to 70°C overnight, equilibrium **3** shifts back toward the left, as shown by an increased **3**:**1** ratio in the $^1\text{H-NMR}$ spectrum. This shows that equilibrium **3** corresponds to an exothermic process. No significant formation of compound **2** is observed under a H_2 atmosphere at room temperature over 2 weeks. After long reaction times, a H/D exchange process with the solvent was also observed (*vide infra*). Representative $^1\text{H-NMR}$ spectra of this reaction in the hydride region are shown in Figure 1.

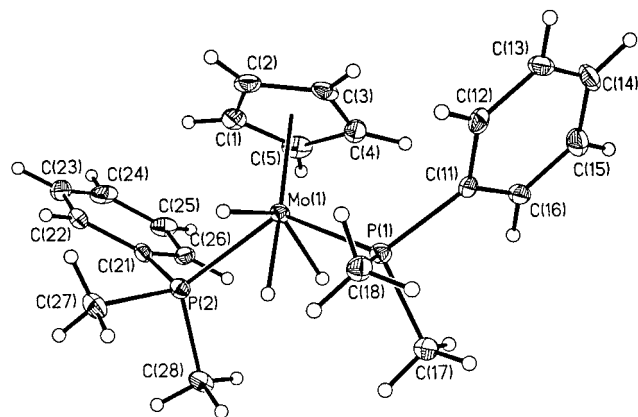


Figure 2. ORTEP view of compound **1** with the numbering scheme used. The ellipsoids are shown at the 30% probability level.

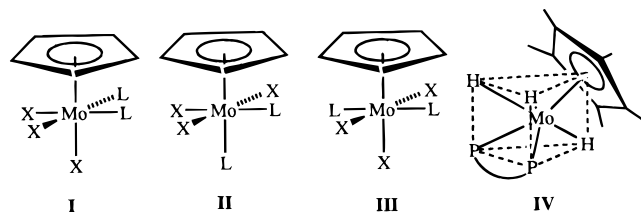
Table 3. Longitudinal Relaxation Times, T_1 , for Compounds **1** and **3** at Various Temperatures

T (K)	T_1 (ms)	
	1	3
205	520	
215	340	
225	282	
235	325	600
245	345	580
260	460	735

The conversion of the ortho-metalated $\text{CpMo}(\sigma\text{-C}_6\text{H}_4\text{-PMe}_2)(\text{PMe}_2\text{Ph})_2$ complex to the monohydride intermediate probably involves a preliminary loss of phosphine, followed by oxidative addition of H_2 and reductive elimination to form the intermediate $\text{CpMoH}(\text{PMe}_2\text{Ph})_2$, as indicated in Scheme 1. This species can either add PMe_2Ph to form the $\text{CpMoH}(\text{PMe}_2\text{Ph})_3$ species or oxidatively add H_2 to afford **1**.

Compound **1** has similar spectroscopic properties to $\text{Cp}^*\text{MoH}_3(\text{dppe})$ ²⁷ and other previously reported trihydrides.⁴⁰ Like all of these previously reported compounds, the hydride resonance does not decoalesce upon cooling to -80°C . The nature of compound **1** as a classical trihydride, rather than as a monohydride-dihydrogen complex, is strongly indicated by the long minimum longitudinal relaxation time, $T_{1\text{min}}$, measured (282 ms at 210 K and 400 MHz). By comparison, the corresponding $T_{1\text{min}}$ value for the monohydride compound **3** is 580 ms at 245 K and 400 MHz. Values of T_1 for compounds **1** and **3** at various temperatures are collected in Table 3.

X-ray Structure. Known molecular structures for compounds of the type CpMoX_3L_2 are pseudo-octahedral with three possible arrangements of the ligands, *fac* (**I**), *mer*, *cis* (**II**), and *mer*, *trans* (**III**). For instance, CpMoCl_3 -



$[\text{P}(\text{OCH}_2)_3\text{CET}]_2$ has structure **I**,²⁸ $\text{CpMoCl}_3(\text{dppe})$ has structure **II**,⁴³ and $\text{CpMoCl}_3(\text{PMe}_2\text{Ph})_2$ has structure

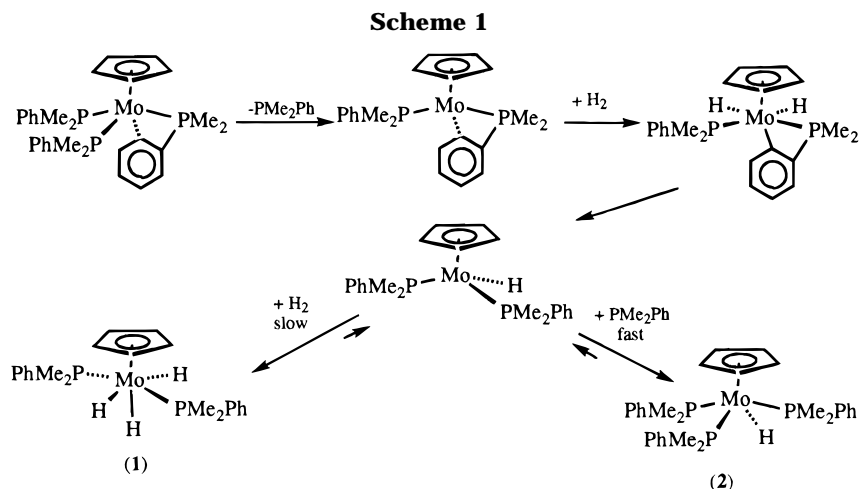


Table 4. Structural Parameters at the RHF Level for $\text{CpMoH}_3(\text{PMe}_3)$

	I	II ^a	III ^a	IV ^a
Mo–C	2.449	2.414	2.462	2.469
C–C	1.432	1.432	1.431	1.433
Mo–H1	1.685	1.679	1.665	1.748
Mo–H2,3	1.707	1.748	1.741	1.710
Mo–P1	2.624	2.651	2.597	2.591
Mo–P2	2.624	2.710	2.597	2.591
CNT–Mo–H1	171.4	97.0	180.0 ^{b,c}	106.9
CNT–Mo–H2,3	101.8	108.7	112.2	110.0
CNT–Mo–P1	114.0	160.7	109.9	120.2
CNT–Mo–P2	114.0	109.0	109.9	120.2
P1–Mo–P2	99.0	90.0	140.0	113.8
C1–CNT–Mo–H1	0.0 ^c	0.0 ^c	0.0 ^c	0.0 ^c
C1–CNT–Mo–H2,3	–80.2	±88.5	0.0, ^c 180.0 ^c	±150.6
C1–CNT–Mo–P1	86.9	0.0 ^b	89.2	75.8
C1–CNT–Mo–P2	–165.6	180.0	–89.2	–75.8

^a Geometries were optimized in C_s symmetry. ^b Ligand is axial to the center of the Cp ring. ^c Parameter constrained in optimization.

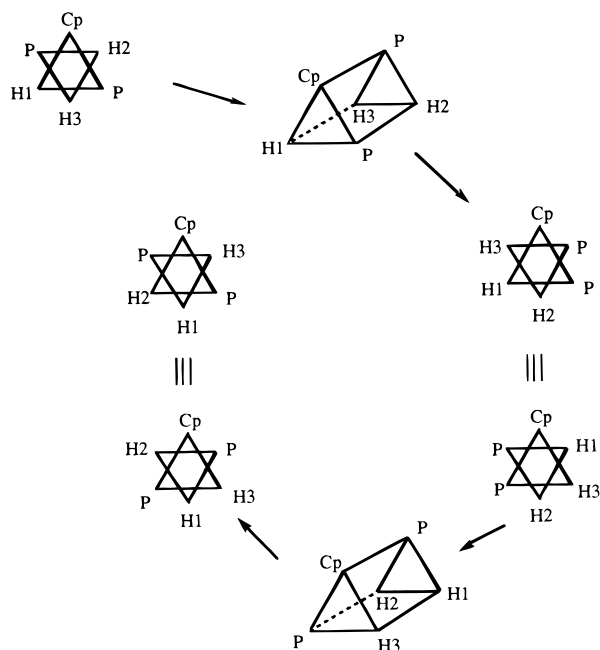
Table 5. Relative Energies of $\text{CpMoH}_3(\text{PMe}_3)_2$ (I–IV) from the RHF Optimized Geometry

structure	RHF//RHF	MP2//RHF
I	4.77	2.92
II	18.96	14.74
III	0.00	0.00
IV	11.23	11.66

III.⁴⁴ However, the only structure so far reported for a trihydride species having this stoichiometry, e.g., $\text{Cp}^*\text{MoH}_3(\text{dppe})$,²⁷ is yet of a different and novel type, e.g., based on the trigonal prismatic geometry, IV.

In order to understand whether the unusual structural preference of $\text{Cp}^*\text{MoH}_3(\text{dppe})$ is due to electronic or steric factors, we have determined the structure of the less sterically crowded compound **1**. The molecular geometry is shown in Figure 2. The three hydrides were directly located from the difference Fourier synthesis and refined without constraints. The geometry can be described as a distorted octahedron with two phosphines trans to one another, two hydrides trans to one another, and the third hydride trans to the Cp ring, e.g., type III, just like the trichloride analogue $\text{CpMoCl}_3(\text{PMe}_2\text{Ph})_2$.⁴² The two $\text{CpMoX}_3(\text{PMe}_2\text{Ph})_2$ ($X = \text{H}, \text{Cl}$) compounds experience significantly different distortions from the ideal octahedral geometry. In particular, the

Scheme 2

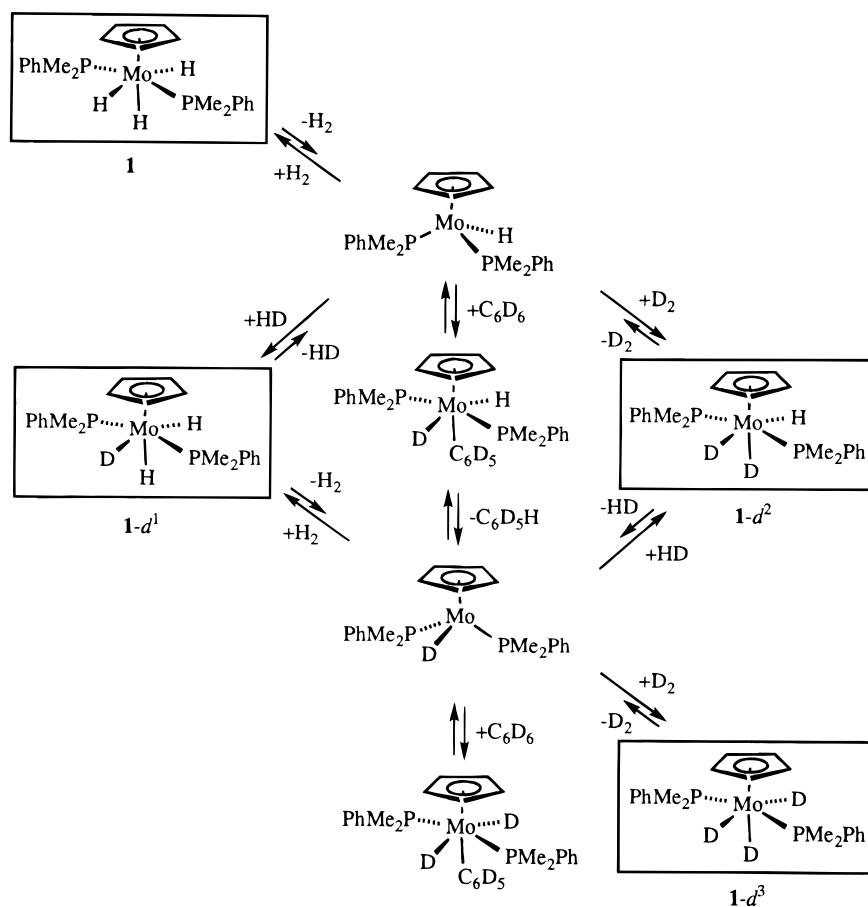


two hydrides in the title compound are much further from the pseudo-equatorial plane (CNT–Mo–H, 111.4(14)° and 112(2)°) with respect to the corresponding chlorides in the structure of $\text{CpMoCl}_3(\text{PMe}_2\text{Ph})_2$ (CNT–Mo–Cl, 99.5(1)° and 104.5(1)°). Correspondingly, the two phosphine ligands are distorted to a greater extent in the trihydride structure (CNT–Mo–P, 116.5(1)° and 117.0(1)°) with respect to the trichloride structure (105.8(1)° and 103.4(1)°). These phenomena are probably associated with relieved steric $X\cdots X$ and $X\cdots \text{PMe}_2\text{Ph}$ repulsions upon changing Cl to H. The conformation of the phosphine ligands is identical in the two structures, with the phenyl rings pointing toward the Cp ring. The Mo–P distances in **1**, however, compare better with those in the pseudo trigonal prismatic complex $\text{Cp}^*\text{MoH}_3(\text{dppe})$ (average 2.37(1) Å)²⁷ than with those in $\text{CpMoCl}_3(\text{PMe}_2\text{Ph})_2$ (average 2.554(1) Å).⁴⁴ Thus, this structural parameter is more sensitive to the Cl/H substitution than to the molecular geometry. The average Mo–H distance of 1.64(4) Å in **1** compares with the previously reported value of 1.59(5) for $\text{Cp}^*\text{MoH}_3(\text{dppe})$.²⁷ The closest H \cdots H contact is 1.79 Å, further confirming the nature of the compound as a classical hydride.

(43) Stärker, K.; Curtis, M. D. *Inorg. Chem.* **1985**, *24*, 3006–3010.

(44) Abugideiri, F.; Keogh, D. W.; Poli, R. *J. Chem. Soc., Chem. Commun.* **1994**, 2317–2318.

Scheme 3



The adoption of a geometry related to **III** for compound **1** strongly suggests that the previously reported structure of $\text{Cp}^*\text{MoH}_3(\text{dppe})$ ²⁷ (e.g., **IV**) is sterically enforced. However, neither structure **III**, structure **IV**, nor the other possible structures **I** and **II** would lead to equivalent hydride ligands. Thus, the measurement of a single hydride resonance for all known compounds of this stoichiometry can only be attributed to high fluxionality. We have previously proposed that the mechanism of hydride scrambling in this class of compounds could take place via a facile interconversion between the pseudo-octahedral and the pseudo trigonal bipyramidal structure.²⁷ Furthermore, recent calculations⁴⁵ on CpOsH_5 show that the hydride scrambling occurs by a trigonal twist. Theoretical calculations, the results of which are shown in the next paragraph, support this proposal for the complexes studied here.

Theoretical Calculations. The geometries of the four structures (**I–IV**) were optimized with $X = \text{H}$ and $L = \text{PMe}_3$ at the RHF levels maintaining C_s symmetry, except for **I** (C_1). Each of the structures were constrained to keep one of the hydride ligands eclipsed with one of the carbons in the Cp ring. Additionally, the phosphine ligands were constrained to possess a C_3 rotational axis and the Cp ring is kept planar. The geometric parameters are provided in Table 4, and the relative energies are listed in Table 5.

The hydride and phosphine ligands in these complexes are bent away from the Cp ring at larger angles than might be expected. This effect is due to a pseudo-

second-order Jahn–Teller (PSOJT) effect⁴⁶ in which these predominately σ -bound ligands bend in order to increase their overlap with the d orbitals of the metal.^{45,47,48} Thus, the ligands are not *cis* or *trans* in the usual sense of a ligand being at right angles or directly across each other. However, that nomenclature is utilized here in reference to the relative dihedral angle with the centroid of the Cp ring. Relative dihedral angles of close to 90° are referred to as *cis* and relative dihedral angles of close to 180° are referred to as *trans*.

A major factor in the stability of structures **I–III** is the proximity of the phosphine ligands. Structure **III** has the lowest energy conformation because the large P–Mo–P bond angle minimizes the steric crowding of the PMe_3 ligands. Thus, this structure is the low-energy conformer in both the calculation and experiment. Overall, the theoretical geometry fits well with the experiment. However, since RHF calculations predict bond lengths that are longer than expected, the large difference in P–Mo–P bond angles between theory and experiment can be attributed to the lengthened Mo–Cp distance, which would allow the bond angle to open up.

Structure **I** might be expected to have the next lowest energy as the equatorial phosphine ligands can adjust their dihedral angle (P–Mo–Cp–C) so that they are farther apart. Interactions of the methyl groups on the phosphines with the Cp ring also destabilize this

(46) Albright, T. A.; Burdett, J. K.; Whangbo, M. *Orbital Interactions in Chemistry*; John Wiley: New York, 1985.

(47) Lin, Z.; Hall, M. B. *Organometallics* **1993**, *12*, 4046–4050.

(48) Bayse, C. A.; Hall, M. B. *Inorg. Chim. Acta*, in press.

(45) Bayse, C. A.; Couty, M.; Hall, M. B. *J. Am. Chem. Soc.* **1996**, *118*, 8916.

structure, with the destabilization more pronounced if Cp* is involved. Structure **II** is the most unstable as the PSOJT effects discussed above force a P–Mo–P angle that would be significantly smaller than 90° if the axial phosphine remained stationary. The optimization compensates for this by moving the axial phosphine 20° off the axis to a final P–Mo–P angle of 90°. The trigonal prismatic structure **IV** roughly corresponds to the previously synthesized Cp*MoH₃(dppe), where the P–Mo–P angle is larger and the CNT–Mo–P angles are smaller than the experimental values, as there are no constraints due to a ethylene linkage between the phosphines. The high relative energy of this conformer is due to the small P–Mo–P angle and to the stability of the pseudo-octahedral geometry for this type of complex.⁴⁵

In light of recent studies on the CpOsH₅ system,⁴⁵ a trigonal twist mechanism is likely for the exchange in this system (Scheme 2). Since structure **II** is very high in energy, it is most likely that the exchange route would proceed through structures **I** and **III** by various trigonal prismatic transition states. Further theoretical work is being performed on these systems and will be presented at a later date.

H/D Exchange in C₆D₆. As mentioned above, the ¹H-NMR monitoring of the reaction between the ortho-metalated complex CpMo(*o*-C₆H₄PMe₂)(PMe₂Ph)₂ and H₂ in C₆D₆, which generated compound **1**, provided evidence for solvent C–D bond activation and H/D exchange. The development of both CpMoH₂D(PMe₂Ph)₂ ($\delta = 5.20$, $J_{\text{PH}} = 40.4$ Hz) and CpMoHD₂(PMe₂Ph)₂ ($\delta = -5.24$, $J_{\text{PH}} = 39.7$ Hz) as flanking triplets to the triplet hydride resonance of **1** is shown in Figure 1. Compound **1-d₂** accumulates to observable amounts only upon UV irradiation of the solution. The irradiation also induces phosphine loss from **1** with formation of the pentahydride complex **3**, as evidenced by the doublet centered at $\delta -4.2$, and the formation of yet another bisphosphine complex, characterized by a broad triplet at $\delta -4.7$, which remains currently unassigned. The growth of the C₆D₅H resonance occurs simultaneously with the growth of the triplets due to the partially deuterated species. Further evidence for H/D exchange was observed in the ²H-NMR spectrum of the above mixture.

These phenomena can be accounted for by reductive elimination of H₂ from **1** to generate CpMo(PMe₂Ph)₂H, which then engages in oxidative addition/reductive elimination processes with the deuterated solvent as shown in Scheme 3. Compound **1-d₁** is obtained directly by oxidative addition of H₂ to the 16-electron CpMoD-(PMe₂Ph)₂ intermediate, whereas **1-d₂** can be obtained by addition of HD to the same intermediate or by

addition of D₂ to CpMoH(PMe₂Ph)₂. HD and D₂ are available from the reductive elimination processes of **1-d₁** and **1-d₂**, respectively. A similar process was also described for (η^5 -C₅H₄Pr¹)MoH₃L₂ (L = PMe₃ or L₂ = dmpe).⁴¹ However, H/D exchange in C₆D₆ was observed only upon UV irradiation for those systems, and the measurement of an isotopic shift for the ¹H-NMR spectra of (η^5 -C₅H₄Pr¹)MoH₃D_{3-n}L₂ was not reported. Small upfield shifts upon H/D isotopic substitution are typical of polyhydride compounds, while the absence of a temperature dependence on the $\Delta\delta$ between different isotopes indicates the absence of an isotopic perturbation of degeneracy,^{49,50} in further agreement with the classical nature of the trihydride molecule.

Conclusions

Compound **1** is only the second compound in the class of complexes (ring)MoH₃L₂ (ring = Cp or substituted derivative) that has been determined structurally. Its structure is based on the octahedron with *trans,mer* stereochemistry (**III**), unlike the previously structurally characterized Cp*MoH₃(dppe) which adopts a trigonal prismatic structure (**IV**). Both of these hydrides are highly fluxional in solution, even at -80 °C. Theoretical calculations on the CpMoH₃(PMe₃)₂ model system indicate that the energy difference between the two geometries is small, but suggest that the hydride scrambling mechanism for CpMoH₃(PMe₂Ph)₂ may proceed through the alternative *fac* stereochemistry (**I**), via a pseudo-Bailar twist.

Acknowledgment. For the experimental part of this work, funding by the Department of Energy (Grant No. DEFG059ER14230 to R.P.) is gratefully acknowledged. C.A.B. and M.B.H. would like to thank the National Science Foundation (Grant No. CHE 94-23271) and the Robert A. Welch Foundation (Grant No. A-648) for their support. They also would like to thank the Supercomputer Facility at Texas A&M University for use of their SGI Power Challenge and Cornell Theory Center for time on the IBM SP2.

Supporting Information Available: For CpMoH₃(PMe₂Ph)₂, tables of crystal data and refinement parameters, fractional atomic coordinates, bond distances and angles, anisotropic thermal parameters, and calculated H-atom coordinates (8 pages). Ordering information is available on any current masthead page.

OM9603600

(49) Heinekey, D. M.; Oldham, W. J., Jr. *J. Am. Chem. Soc.* **1994**, *116*, 3137–3138.

(50) Paneque, M.; Poveda, M. L.; Taboada, S. *J. Am. Chem. Soc.* **1994**, *116*, 4519–4520.